POLITECNICO DI TORINO
Repository ISTITUZIONALE

Rockfall in open pit mines: management of the pit geometry and protection measures design

Original
Rockfall in open pit mines: management of the pit geometry and protection measures design / Marchelli, Maddalena; Peila, Daniele; Giacomini, Anna. - In: INTERNATIONAL JOURNAL OF ROCK MECHANICS AND MINING SCIENCES. - ISSN 1365-1609. - 170:(2023), pp. 1-15. [10.1016/j.ijrmms.2023.105551]

Availability:
This version is available at: 11583/2980755 since: 2023-07-28T13:34:04Z

Publisher:
Elsevier

Published
DOI:10.1016/j.ijrmms.2023.105551

Terms of use:

This article is made available under terms and conditions as specified in the corresponding bibliographic description in the repository

Publisher copyright

(Article begins on next page)

20 March 2024

International Journal of Rock Mechanics & Mining Sciences 170 (2023) 105551

Contents lists available at ScienceDirect

International Journal of Rock Mechanics and Mining Sciences

journal homepage: www.elsevier.com/locate/ijrmms

Rockfall in open pit mines: management of the pit geometry and protection measures design

Maddalena Marchelli [a,*], Daniele Peila [a], Anna Giacomini [b]

[a] Department of Environment, Land and Infrastructure Engineering (DIATI)- Politecnico di Torino, C.so Duca degli Abruzzi 24, I–10129 Torino, Italy
[b] Priority Research Centre for Geotechnical Science and Engineering, College of Engineering, Science and Environment, University of Newcastle, University Dr, 2308 Callaghan, NSW, Australia

ARTICLE INFO

Keywords:
Rockfall
Open pit
Trajectory analysis
Design charts

ABSTRACT

Rockfall events represent a serious hazard for people, structures, and infrastructures. The phenomenon can occur in several environments, natural and artificial. In surface mining operations, blasting, bench clean-up and scaling can induce rock blocks detachment, compromising operators' and operations' safety. The installation of passive mitigation measures coupled with a specific design of the pit geometry can mitigate this risk. The bench height, width, and slope angle, the number of benches, together with the material characterizing the slope, affect in different ways the kinematics of the possible detached blocks. In this paper, a large set of configurations is studied and trajectory analyses are performed to evaluate the influence of each geometrical or material variable. Results are analysed considering blocks kinematics both on the pit floor and at each bench. The findings provide a useful a tool for a preliminary design of pit geometry and mitigation measures. Design charts are proposed for different slope materials, reporting, as function of the total pit height, the blocks stopping distance, their velocity at the pit floor, their passing height and velocity at each bench, for each geometrical configuration. The obtained charts can be effectively implemented in a quantitative risk assessment procedure for mining activities.

1. Introduction

Rockfall phenomena are among the most dangerous landslide events, involving the detachment and the consequent rapid movements, i.e. bouncing/rolling/sliding, along a natural or artificial slope of individual rock blocks or rocky fragments ranging from small fragments to massive boulders of tens cubic meters.[1] According to the intensity of the phenomena and to both exposure and characteristics of the elements at risk, serious damages can occur on infrastructures, structures, people and, in working sites, workers and machinery,[2] even at a large-scale. In surface mining, rockfall events can also be affected by unpredicted structural conditions ahead of mining and variations in planned slope designs (and related geometries) upon optimization of drill and blast operations, exposing workers, machinery, and site equipment to unpredicted risks. Pre-mining activities, bench cleanup and scaling, and blast activities can further enhance block detachments and rockfall phenomena.[3,4] In areas exposed to extreme meteorological events, natural weathering, freeze-thaw actions and intense rainfall can further contribute to an inaccurate design of blasting or scaling operations for both the intermediate and the final configurations.[5,6] Rockfall risk mitigation is a fundamental requirement for safe operations, reducing the risk of unexpected work interruptions and, thus, substantial economic losses.[7] Several rockfall hazard[8–10] and risk[11–13] assessment methods have been proposed over the last few decades to assess the level of the hazard, to quantify the severity of the damages and to increase activities safety in resource exploitation. The installation of various mitigation solutions has significantly increased over the last decade to respond to the risks posed by rockfalls[14–20]: drapery meshes, waste rock and/or engineered embankments and net fences are widely adopted in surface exploitation of various rock materials. Novel monitoring procedures and technologies can also provide accurate data on event magnitude and return period, allowing detailed catalogue of events, their characteristics and possible triggering conditions, to be collected.[21–25]

Besides protection and mitigation works, rockfall hazard in open pit mines can be primarily controlled through bench design.[7,26] The geometry of the excavation is generally defined according to a detailed geotechnical model, for which geostructural and hydrogeological features of the rock mass in the pit area have been thoroughly investigated through field and, possibly, laboratory tests. Stratification, schistosity and discontinuity sets impose limits to the height, width and slope of

* Corresponding author.
E-mail address: maddalena.marchelli@polito.it (M. Marchelli).

https://doi.org/10.1016/j.ijrmms.2023.105551
Received 13 January 2023; Received in revised form 9 June 2023; Accepted 11 July 2023
1365-1609/© 2023 The Author(s). Published by Elsevier Ltd. This is an open access article under the CC BY license (http://creativecommons.org/licenses/by/4.0/).

the steps.[5,27–29] As rockfall can originate during operations even in apparently stable zones,[6] a thorough understanding of rockfall kinematics in terms of trajectories, velocities, rebounds and run-out distance is indeed a priority in the decision-making processes for exploitation and for the design of mitigation measures.[30]

Several experimental and numerical studies[31–36] have been conducted in open pit mining contexts to perform an effective design of either (i) the slope configuration, i.e. the geometric arrangement of the benches on the pit wall, to avoid rockfall propagation or (ii) the protective mitigation measures for a given geometry. Single or multiple benches slope geometries have been considered and a number of charts (or design suggestions) has been proposed. Nevertheless, these studies have considered the contribution of rockfall mitigation for a single bench geometry, only.[31,32,36] A tentative of including multiple benches has been proposed,[34,35] with the aim of defining the best geometry that limits (but not to completely remove) the risk. In this last case, neglecting rockfall trajectory analyses specific for a given open pit site,[37–39] the literature does not provide rockfall parametric analyses evaluating for each bench and at the pit floor the kinematic parameters of the possible falling blocks during their motion. Section 1.1 provides the main results of the above mentioned studies. Hence, coupled scenarios, i.e. multiple benches with mitigation measures, are completely missing.

The present works aims at providing an useful tool for the effective design, in reference to rockfall hazard, of both (i) pit slope and (ii) mitigation measures, considering single or multiple benches configurations. To achieve such goal, several parametric rockfall trajectory analyses in a hypothetical open pit are performed and analysed, considering different possible geometries and slope outcropping materials. Blocks run-out and kinematic parameters at each bench are investigated. Pit geometries and materials typical of European rock exploitation (Fig. 1(a) and (b)) and Australian coal mine environments are considered.

Several analyses were conducted. First, the configurations that minimize the number of blocks arriving at the pit floor were analysed together with the parameters that mostly affect the results in terms of arrival probability, distance, and velocity. Since avoiding or minimizing the number of arriving blocks at the pit floor is not always achievable or affordable, the kinematic characteristics of falling blocks at each bench were investigated. To provide a tool for a preliminary design of both pit geometry and mitigation measures, four design charts were produced for each of the investigated slope materials, reporting the characteristic values of the kinematic parameters of the blocks at each bench and at the pit floor. These charts can also be implemented in quantitative risk assessment methods tailored for open pit, as the one proposed by Alejano et al.[11] or Peila et al..[13]

Section 2 presents the proposed methodology, the input parameters and the performed analyses, while Section 3 deals with results: a deep analysis of blocks reach probability and their impacts at the pit floor are provided in Section 3.1, while blocks kinematics at each bench are addressed in Section 3.2. Section 3.3 presents the above mentioned design charts with an example of use. Finally conclusions and future perspectives are outlined in Section 4.

1.1. Previous studies

As previously stated, issues related to pit design optimization against rockfall hazard have been tackled by few Authors. Even not finalized for open pit design, only, it is worth mentioning the pioneering study conducted by Ritchie,[31] whose work included the rolling of hundreds of rocks off state-owned quarries and talus slopes across Washington state (US). The paths and the distances of the falling blocks were recorded and measured. The work led to the definition of an empirical method for roadway ditch design, to prevent falling rocks from reaching the travelled area of a road, proposing a set of practical design criteria further collected in a chart. For the particular open pit case, these results can be adopted for investigating blocks dynamic in a single bench geometry. Nevertheless, the chart provides the geometry

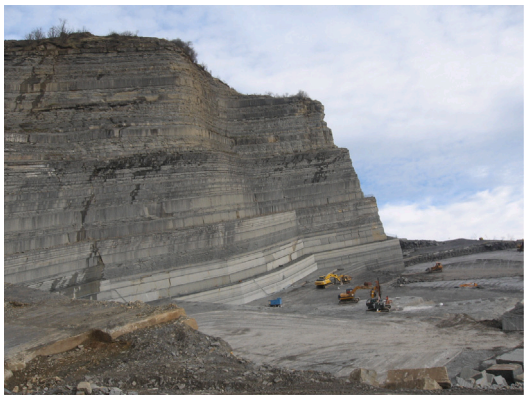

(a)

(b)

Fig. 1. Sandstone quarry in Fiorenzuola, Italy (a), and aggregate quarry in Pedogna, Italy (b). Courtesy of Prof. M. Coli.

of a catchment area for a 100% (total) retention of blocks, not considering variable retention levels for a cost/benefit design approach. Moreover, the proposed catchment ditch solution was not feasible in all the cases. Consequently, thanks to an extensive campaign of field tests, Pierson et al.[32] investigated how slope, catchment area and rockfall properties affect the rockfall retention. The Authors developed guidelines, including design charts, for partial retention of blocks with also flat catchment area. Also in this case, the work was not specifically targeted to open pit design but, as tests were performed in such context, the results were used also for single bench design. Evans[40] reached similar results through real tests in mine benches. Call, in Ref. 27, specifically focused on rockfall hazard in open-pit mines and in the optimization of bench and catch-ditch design from a cost perspective compatible with safety standard. Defining the excavation of a ditch as not practical and substituting the ditch with a berm, Call proposed to improve Ritchie's criterion applied to mining, with a minimum bench width $b_{w,min}$ equal to:

$$b_{w,min} = 1.2 + 0.2b_h \quad \text{(m)}, \tag{1}$$

where b_h is the bench height (in meters). The suitability of this formula was confirmed by Ryan and Pryor,[26] even though a reliability based approach to evaluate bench slopes was then proposed where a variability in geologic structure makes difficult to have a constant inter-ramp slope angle. The approach considered different issues and was not only targeted to rockfall hazard but required an amount of input data often difficult to achieve.

The first study on rockfall hazard on multiple benches in open pit mines was performed by Peila et al..[34] The Authors investigated, with their own 2D lumped-mass trajectory code, the specific configuration

of four benches, 15 m high, 2.5 and 5 m wide. With a first attempt to insert fragmentation, the Authors analysed 9 different combinations of normal and tangential restitution coefficients and friction angle, different bench-by-bench. Despite no design charts were developed, interesting design tips were suggested: (i) reduced bench slope tends to project rock blocks at a greater distance, with a prevailing horizontal direction; (ii) for very steep bench inclination, a slight increase of bench width does not vary the results; (iii) as a preliminary rockfall mitigation measure, debris could be distributed on the bench.

Starting from all the above mentioned references, Alejano et al.[35] performed numerical trajectory analyses on synthetic 2D profiles, representative of hard-rock quarries, investigating the influence of the geometrical parameters in the falling block retention capacity at the pit floor. A lumped-mass approach was adopted (RocFall code), performing simulation for 2, 5 and 8 benches slopes, bench inclinations of 2:1, 3:1, and 4:1, and bench heights spanning up to 25 m, back-calculating the catch-bench widths able to retain 75%, 90%, and 95% of the blocks. A unique set of input parameters that describe rock-slope interaction was considered, with a slope roughness, i.e. a variability of the angle at the point of the impact, of 0.1 in standard deviation. This set was considered as representative of hard-rock quarry and results were organized in design charts. Nevertheless, to assess the sensitivity of results to different input data, parametric studies were performed for a series of particular cases, and the mean values for the restitution coefficients and slope angle were proved to be the most significant parameters.

More recently, Ferrari et al.[36] conducted rockfall sensitivity analyses on a 2D synthetic profile, representative of a rock cliff (or a single bench configuration). A lumped-mass model was adopted and RocFall code was used for the simulations. Height (from 5 m to 100 m) and slope angle (from 50° to 85°) were varied, together with restitution coefficients, friction angle and slope roughness. The first impact location and velocity were investigated. In a probabilistic framework, the $95th$ and the $90th$ percentiles for arrival and velocity, respectively, were considered as representative. Thanks to the properties of the selected trajectory model, the kinetic energy can be derived from the known mass of the falling block. Fitting the obtained data applying a linear regression through the origin, empirical equations were proposed for the preliminary calculations of the first impact position and the kinetic energy as function of the slope height, inclination and irregularity of the rock face, subdivided in classes. On the basis of this study, a qualitative rockfall hazard assessment procedure for highwall was developed.[10] From a known state of activity of the highwall, i.e. describing rockfall frequency, together with the expected rockfall energy, a level of hazard could be defined. The knowledge of the first arrival is instead used for locating workers, machinery and infrastructures over the working areas at the toe of highwalls.

2. Methodology

An adequate design of catching benches in open pit mines is fundamental to prevent and/or minimize rocks detached in the upper portions of the pit slope from reaching working areas located at the pit floor, where workers and equipment are located. A balance between optimum design and production rate needs to be explored[5,41] and, when necessary, the installation of protective measures should be considered. Several parametric trajectory analyses were performed within a probabilistic framework with the precise aim of evaluating (i) which geometrical configurations can provide an acceptable level of risk, i.e. blocks are unlikely to arrive on the pit floor, and (ii) which performances are required to the protective measures installed on the intermediate benches.

Starting from the indefinite slope assumption, which holds for wide excavation sites, and following what proposed by Refs. 35, 36, trajectory analyses on 2D synthetic profiles were performed. The heterogeneity of site conditions in term of materials was accounted thanks to a selection of normal and tangential restitution coefficients (Section 2.2). A lumped-mass approach was selected as the most suitable to compare various profiles with different materials and geometries. In addition, the adoption of a point-mass model, in which trajectories are not affected by the block mass, allows scaling the results in terms of kinetic energy according to the mass.[36] A very large number of trajectory analyses was performed to analyse all these variables: 384 different geometries with 12 different materials pairs, i.e. 4608 configurations. The need of performing such a number of analyses, recording and managing all the output quantities, underlies the choice to develop a specific trajectory code on Matlab (R2021b) environment, mimicking RocFall software (RocScience Suite).[42] The code was validated by comparing the results on a sample slope with those obtained from RocFall 2019,[42] as detailed in Appendix A.

To encompass the uncertainties associated with the rockfall phenomenon,[43] as suggested by the Eurocodes,[44,45] trajectory analyses are performed in a probabilistic framework: at each bench, blocks passing height and velocity are recorded together with the stopping distance and the impact velocity at the pit floor. This approach promotes the design of protective measure. Following Eurocode 0,[44] the structural works have to be designed through a partial safety factors design approach, where the effect of actions, i.e. the kinematic parameters of the blocks, are expressed through reference, or characteristic, values (determined from the probability distributions). Considering the suggestions provided by the Italian Standards for rockfall protective measures UNI 11211-4,[46] widely adopted in Europe, and coherent with Eurocode 7,[45] the $95th$ percentile of the distributions can be chosen as characteristic value. Design values of the variables are obtained by multiplying the characteristic values times the partial safety factors.

Table 1
Considered layouts for the trajectory analyses.

Parameter	Value
bench face height b_h (m)	10, 20, 30, 40
bench width b_w (m)	3, 5, 7
bench face slope β (°)	50°, 60°, 70°, 80°
number of benches n_b (–)	1, 2, 3, 4, 5, 6, 7, 8

2.1. Slope geometry

Different layouts were considered for the 2D synthetic profiles were performed, trying to encompass the great majority of the cases. In open pit with several benches, a bench height b_h usually ranges between 10 m and 20 m.[5] In particular contexts, e.g. in Australia, benches with a height spanning from 20 to 40–50 m with few steps can be observed. Referring to bench width b_w, the most adopted size is 7 m, although smaller values can be found in transitory or final dismantling configurations.[34] Bench face angle, which is controlled by the intersecting joints and faults, typically spans from 50° to 80–85°.[5,7]

To account for a large set of configurations, the analysis was conducted considering (i) the possible number of benches ranges from 1 to 8, (ii) three bench widths (3, 5 and 7 m), (iii) four bench heights (10 to 40 m) and (iv) four bench face slopes (from 50° to 80°). Table 1 summarizes the studied configurations.

Assuming a 2D regular profile, it should be noted that the present work does not tackle with the backbreak along the top of the bench issue, i.e. the horizontal distance between a planned and a real bench crest.[47]

2.2. Slope material

With the leading idea to create charts for the preliminary design of both open pit geometry and mitigation/protection works, for each possible extraction site, different materials were considered. As stated in Section 1, the parameters governing the interaction between a

Table 2
Values of the input parameters related to the block-open pit interaction. The subscript m accounts for the mean value of the parameters. It is worth mentioning that the maximum R_n and R_t is set to 1.0 in the Monte-Carlo sampling process.

Parameter	Value
$R_{n,m}$ (–)	0.3, 0.4, 0.5
$R_{t,m}$ (–)	0.35, 0.55, 0.75, 0.85
ϕ_m (°)	30°
σ_n (–)	0.03
σ_t (–)	0.03
σ_ϕ (°)	1°
Roughness (°)	±1°

block and the terrain along which it moves are the normal restitution coefficient R_n, the tangential restitution coefficient R_t, and the friction angle ϕ. While the first and the second stand for block energy loss during bouncing, the friction angle accounts for energy dissipation of the block during its roto-translational motion along the path. Although all these parameters are influenced by the shape and the geomechanical characteristics of both the block and the terrain, together with the velocity and orientation of the block at the impact,[48] in a lumped-mass model the value of the parameters is mainly material-dependent. As often adopted, a unique friction angle $\phi = 30°$ was assumed.[36] Following these considerations, hereafter, the Authors use the term *material* to indicate a couple of R_n and R_t values.

Considering the ranges suggested in the literature for rocky outcrops, R_n generally spans from 0.30 to 0.50 and R_t from 0.65 to 0.9,[16,33,49–54] taking specifically into account simulations performed with lumped-mass 2D model.[42,55] For specific cases, Refs. 16, 36 found that R_t can reach 0.35.

To account for a large set of materials, the analysis was conducted considering that (i) the normal restitution coefficient R_n ranges from 0.3 to 0.5, (ii) the tangential restitution coefficient R_t ranges from 0.35 to 0.85 and (iii) a unique friction angle $\phi = 30°$ is assumed. As further detailed in the following section, in a probabilistic framework these represent the mean values of material parameters identified with $_m$ subscript. For a simplified and conservative assumption, and for having an overview of general validity, an homogeneous material was assumed for the whole profile, neglecting thus the presence of debris on the benches or particular situations that can be developed in future studies.

2.3. Trajectory analyses

As in a probabilistic approach, the performed trajectory analyses consist in a set of throws, i.e. simulations, from the individuated source area, in which the input parameters related to the material are randomly selected in a predefined range. Random sampling approaches should be based on theoretical knowledge for all the probabilistic parameters. In the case of the restitution coefficients, Gaussian and uniform distribution represent the most adopted distributions, even though currently there is no evidence that the values in a range have equal probabilities or conform to other types of probability distribution.[43,56,57] In the present work, a Gaussian distribution was assigned, as already performed by Alejano et al.,[35] Ferrari et al.,[36] and Frattini et al..[58] The mean values correspond to $R_{n,m}$, $R_{t,m}$, and ϕ_m, while the standard deviations are σ_n, σ_t, and σ_ϕ, respectively.

Table 2 reports the values adopted in the simulations, resulting in $3 \times 4 = 12$ combinations of $R_{n,m}$, and $R_{t,m}$. Since it was intended to represent widely different materials, a narrow Gaussian distribution is assumed, i.e. low values of σ_n and σ_t, following the findings of Chau et al.,[52] who experienced standard deviations from 1% to 15%, but generally less than 5%, and of Asteriou et al..[48]

To account for a possible slight variability in the local surface angle of segments of the slope, a slope roughness was considered, i.e. allowing a variation of ±1° to the angle at the point of the impact.

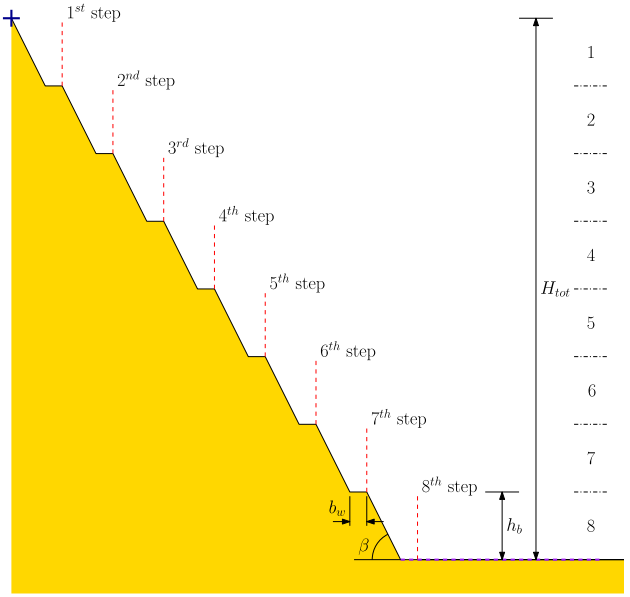

Fig. 2. Scheme of a considered synthetic profile used for the trajectory analyses. The sketch reports a 8 steps configurations. Blue cross represents the source area, while red and the purple dashed lines the vertical and the horizontal collectors, respectively.

As the number of simulations for each configuration should be sufficiently large to guarantee the statistical significance of the results, 6000 throws were performed in each of the considered configurations. Even though rockfalls may start anywhere along the slope, their occurrence is more common from the upper part of the benches.[35] Hence, the detachments of blocks from the top of the pit was considered, with a non-null, but low, initial velocity (i.e. 1 m/s) to mimic the trigger conditions related to external agents. A number of collectors, or not-physical sections in which the kinematic parameters of the blocks are recorded, were considered according to a potential suitable location of mitigation measures. In particular, 1 to 8 vertical sections on the steps represent the possible locations for the installation of passive measures, while a horizontal section at the pit bottom was considered to record the run-out distances of the blocks, together with their velocity at the impact (Fig. 2). Under lumped-mass assumption, blocks velocity was considered to implicitly account for kinetic energy, as, known the mass m_b of the possible impacting blocks, energy can be derived as $E = \frac{1}{2} m_b v^2$. Thus, in the vertical sections, the height of the trajectory, h, and the velocity of the blocks, v_v, were recorded. In the horizontal section, the run-out distance, d, and the impact velocity, v_h, were measured.

3. Results and discussion

This section details the results of the propagation analyses. First, the probability of reach and blocks kinematics at the pit floor were investigated, individuating the geometrical parameters and the materials, i.e. the couples $R_{n,m}$ and $R_{t,m}$, which minimize the numbers of arriving trajectories and the distance, together with the velocity. The velocity of the falling blocks impacting on the pit floor is indeed fundamental to evaluate the kinetic energy and, thus, the degree of damages on workers and infrastructures. Second, since a specific geometry cannot be implemented, protective measures can be required to prevent blocks impacting on the floor, or on the working benches. For this reason, the knowledge of passing height and velocity at each bench was evaluated and trends analysed.

Following Eurocode 0 design principles, the 95th percentiles of the distributions of the output quantities are considered as the characteristic values of the output variables. The results, grouped for each material, were presented, for each layout, in terms of:

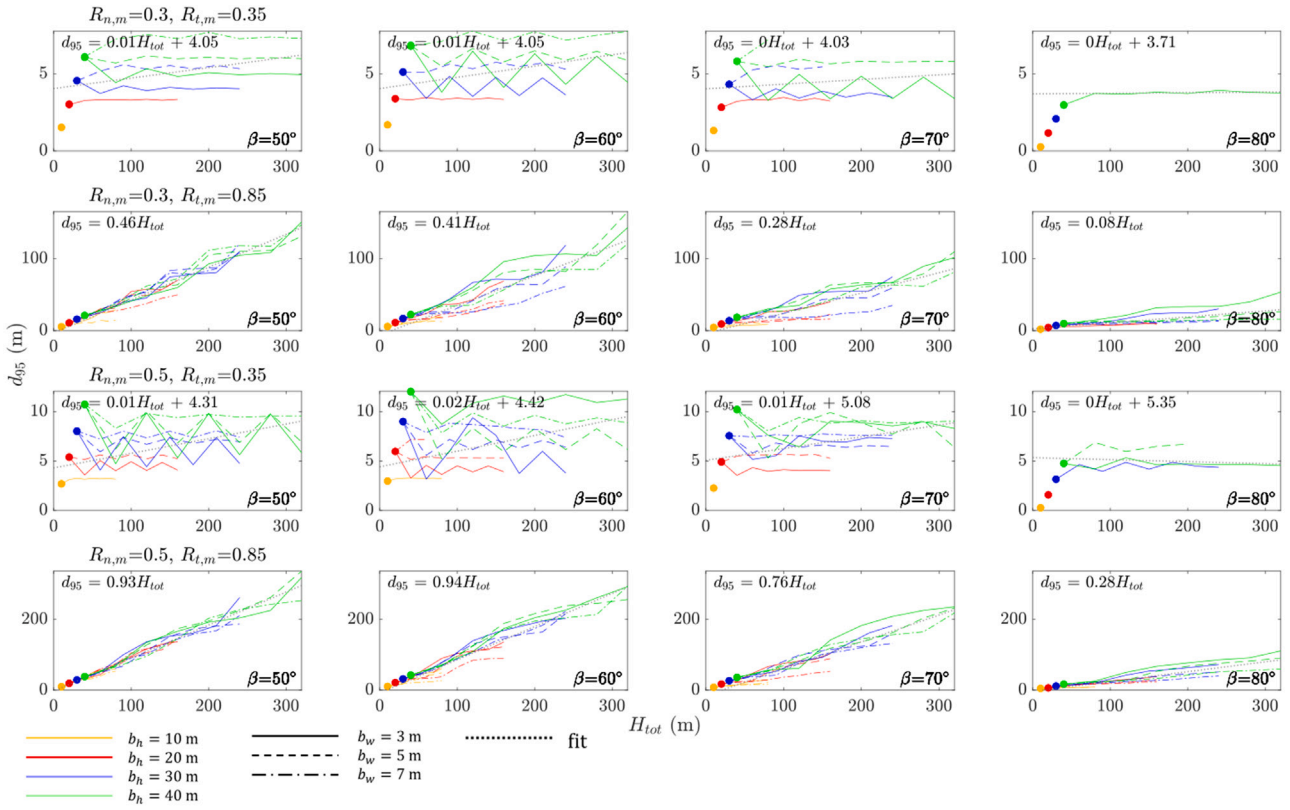

Fig. 3. Values of d_{95} for different couples of $R_{n,m}$ and $R_{t,m}$, grouped for different values of β. Details of the plots are reported in the text.

- run-out distance of the blocks on the pit floor, d_{95};
- velocity of the blocks when impacting on the horizontal pit floor, $v_{h,95}$;
- passing height of the blocks recorded on each vertical section, h_{95};
- velocity of the blocks recorded on each vertical section, $v_{v,95}$.

3.1. Rockfall hazard on pit floor

Fig. 3 displays the run-out distance of the blocks on the pit floor, d_{95}, for the four extreme value pairs of $R_{n,m}$ and $R_{t,m}$, i.e. with minimum and maximum values of both parameters. Each material condition is reported in the row of the plot; the graphs are grouped for β values (columns of the plot). In the x-axis, the total height of the pit H_{tot} is indicated. Different colours and line types are used to indicate b_h and b_w values, respectively, as displayed in the legend. The number of benches is thus univocally determined according to H_{tot} and b_h. Coloured bullets indicate geometrical configurations for which blocks arrive only in the case of a single bench (n_b=1).

It could be noticed that for very low values of $R_{t,m}$ (first and third rows), the blocks tend not reach the pit floor (in particular with multiple benches) and the range of d_{95} values remains below 7 or 10 m, increasing $R_{n,m}$. Despite being in the same range and with the similar trend, the bench height b_h has the effect of slightly increasing d_{95}; a similar effect is noted if the bench width b_w reduces. The number of benches n_b does not influence the output. It is worth mentioning that for a bench inclination $\beta = 80°$, blocks arrive on the floor if $b_h = 40$ m and $b_w = 3$ m, only. Neglecting $n_b = 1$, for which unavoidably blocks arrive on the floor, the linear fit the results leads to almost a constant value $d_{95} \sim 4$ m (Fig. 3, dotted line).

For high values of $R_{t,m}$, regardless of $R_{n,m}$ (second and fourth rows), for almost all the geometrical configurations the blocks reach the pit floor, with distances that are positively affected by H_{tot} or, as a consequence, by the total number of benches n_b. For a given β, a fitting is with a straight line through the origin (Fig. 3, dotted line), irrespective of b_h and b_w, is possible and highlighted. The slope of the linear fit is similar for β = 50–60°, while it decreases for higher β, especially for $\beta = 80°$. The value of the slope has also a great variability according to $R_{n,m}$. It is interesting to observe that for $R_{n,m}$ = 0.5 and β = 50°–60° the slope of the fit line is almost equal to one, i.e. d_{95} tends to H_{tot}, while it reduces to almost $0.3H_{tot}$ for $\beta = 80°$.

All these aspects can be explained in terms of trajectories. In case of low tangential restitution coefficient, the falling blocks, once reaching each bench tread, dissipate a great amount of their kinetic energy and continue their motion to the following bench with a trajectory pattern quite similar to the one with which they started their initial fall (Fig. 4.a). In this case, the influence of the number of benches is negligible, as in all the benches similar trajectories occur, even though some blocks stop on some intermediate benches. The higher the bench, the higher the acquired velocity at the impact and, thus, the outgoing velocity and the final value of d_{95}. Increasing b_w, some of the trajectories stop on the first bench. On the contrary, for high $R_{t,m}$, once impacting a bench, the velocity vector of the blocks acquires a tangential component higher than the normal one, and the resulting parabolic motion cannot directly reach the following bench, but the one beyond (Fig. 4.b). The increment in β causes the parabolic motion to prevail on the sliding/rolling one, resulting in an almost vertical impact on bench tread and, thus, in trajectories similar to those for low $R_{t,m}$ values, but with less energy dissipation. The study reveals that low $R_{t,m}$ values and $\beta = 80°$ allow obtaining zero (or negligible) block probability of reach for several configurations in terms of b_h and b_w. It should be noticed that the high d_{95} values obtained in this study are the result that the pit floor is completely free of obstacles and debris. Nevertheless, the knowledge of d_{95} rather than recording the arrival (or not) of the block on the pit floor can provide important information on the level of hazard.

To better analyse the influence of the parameters on both arrival probabilities on the pit floor and d_{95} values, all the results related to the 4608 configurations are statistically organized and summarized into

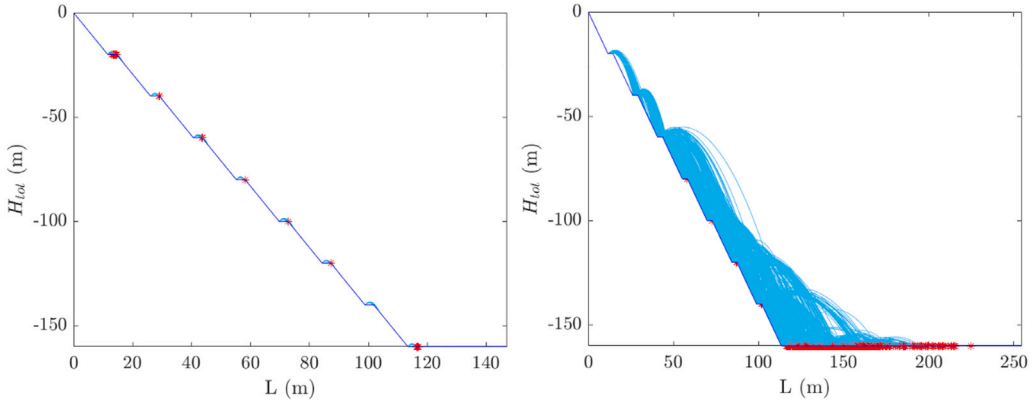

Fig. 4. Results of the trajectory analyses for b_h = 20 m, b_w = 3 m, n_b = 8, β = 60°, for (a) $R_{n,m}$ = 0.30 & $R_{t,m}$ = 0.35 and (b) $R_{n,m}$ = 0.30 & $R_{t,m}$ = 0.85. Red stars indicate blocks stopping points.

Table 3
Maximum values for d_{95} and $v_{h,95}$ recorded at the pit floor for all the configurations.

$R_{n,m}$, $R_{t,m}$	$d_{95,max}$	Geometry of $d_{95,max}$				$v_{h,95,max}$	Geometry of $v_{h,95,max}$			
(–)	(m)	b_h	b_w	β	n_b	(m/s)	b_h	b_w	β	n_b
0.3 , 0.35	7.8	40	7	60°	3	26.5	40	3	80°	2
0.3 , 0.55	13.0	40	5	60°	6	29.5	40	3	70°	2
0.3 , 0.75	93.0	40	3	50°	8	51.1	40	3	60°	8
0.3 , 0.85	165.4	40	5	60°	8	65.8	40	3	60°	8
0.4 , 0.35	9.3	40	3	60°	1	26.5	40	3	80°	2
0.4 , 0.55	17.8	40	3	50°	4	30.2	40	3	70°	2
0.4 , 0.75	148.3	40	3	60°	8	58.5	40	3	70°	7
0.4 , 0.85	243.7	40	3	50°	8	66.7	40	3	60°	8
0.5 , 0.35	12.0	40	5	60°	1	26.5	40	5	80°	2
0.5 , 0.55	40.4	40	3	70°	8	42.9	40	3	70°	5
0.5 , 0.75	212.6	40	5	60°	8	65.4	40	3	70°	8
0.5 , 0.85	336.6	40	5	50°	8	67.6	40	5	60°	8

pivot plots. Fig. 5 displays the percentage of arrivals on the pit floor with respect to the blocks detached, i.e. the arrival or reach probability, subdivided for β and further subdivided in the x-axis according to $R_{t,m}$, which is found to be the relevant parameter. The pivot plots report the data also for the remaining four parameters, i.e. $R_{n,m}$, b_h, b_w, and n_b (Fig. 5.a to d, respectively). In each case, the configurations of the slope are grouped according to the parameters of the x-axis, the mean percentage value is considered.

For a given tangential restitution coefficient, the graph of Fig. 5.a reveals that the increase of $R_{n,m}$ has the effect of increasing the number of arrivals. This trend is less evident if $R_{t,m}$ increases, as the majority of the blocks arrive on the pit floor. The graph highlights an interesting situation: for $R_{t,m} \geq 0.55$, the increase of $R_{n,m}$ involves higher percentages of arrival, while the case $R_{t,m} = 0.35$, for all $R_{n,m}$, displays a higher percentage of arrival than for $R_{t,m} = 0.55$. This trend is more evident in several $R_{n,m}$ and β configurations: for $\beta = 50°$ for $R_{n,m} \geq 0.4$ and for $\beta = 60°$ for $R_{n,m} \leq 0.4$.

Analysing in detail the cases with $R_{t,m} = 0.35$, it results that there are few configurations in which the blocks reach the pit floor, whereas in such scenarios, almost the totality of the throws arrives. Besides, since in the pivot plots the mean value is reported, the resulting figure is low. In $R_{t,m} = 0.55$ it results that there are more configurations in which the blocks reach the pit floor, but with a lower arrival probability. That is why, in general, the bars in the pivot plots of Fig. 5 are shorter or equal to the ones related to $R_{t,m} = 0.35$. Analysing the trajectories, for b_h = 40 m, $b_w \leq 5$ m, and $50° \geq \beta \leq 60°$, in case on $R_{t,m} = 0.55$, a significant percentage of blocks stops at the second bench (see also Fig. 5.b and c): after the first step, bouncing becomes the prevailing motion, instead of sliding as in $R_{t,m} = 0.35$, and, thus, energy dissipates more rapidly.

Both b_h and b_w (Fig. 5.b and .c) influence the results: the decrease of b_h and the increase of b_w has the effect of reducing the number of arrivals. Finally, neglecting $n_b = 1$, for which blocks unavoidably arrive on the pit floor, negligible influence can be observed changing n_b (Fig. 5.d), except for $R_{t,m} = 0.55$ and $n_b = 2$, for which, as observed before, some configurations involve a significant percentage of stopping blocks on the second bench. In the four subplots, the influence of β is negligible except for $\beta = 80°$ (for which a reduced number of arrivals is displayed), while for $\beta = 50°$–$70°$ the results are comparable.

With a similar approach, Fig. 6 reports the pivot charts of the mean (bars) and the maximum (points) values of d_{95}. The y-axis is in logarithmic scale for sake of readability. As in the previous case, the x-axis relates to $R_{t,m}$ and the pivot plots divide the data also for the remaining four parameters, i.e. $R_{n,m}$, b_h, b_w, and n_b. As observed in Fig. 3, and particularly in the fitting lines equations, for $R_{t,m} = 0.35$, the influence of $R_{n,m}$ is almost negligible. Observing Fig. 6.a, the increase of $R_{n,m}$ results in an increase of d_{95}. A similar conclusion can be drawn observing Fig. 6.d where the results are grouped with respect to n_b. A positive correlation can be observed for b_h (Fig. 6.b), while the effect of b_w on the values of d_{95} is negligible (Fig. 6.c). The bench angle does not affect the results, except for $\beta = 80°$, as observed in the previous analyses.

Table 3 reports, for each material, the maximum values of d_{95} together with the correspondent slope geometrical configurations. Confirming the previous observations, all the maximum values are reached with b_h equal to 40 m, the great majority with b_w equal to 3 m and $\beta \sim 50°$–$60°$. No evident trends are observable for n_b, for $R_{t,m} \leq 0.55$.

Fig. 7 displays the velocity of the blocks when impacting on the horizontal pit floor $v_{h,95}$ for the four extreme value pairs of $R_{n,m}$ and $R_{t,m}$, i.e. with minimum and maximum values of both parameters. Each material condition is reported in the row of the plot. The graphs are grouped for β values (columns of the plot), and on the x-axis the total height of the pit H_{tot} is indicated. It is worth mentioning that the velocity refers to the first impact of the block on the pit floor. For

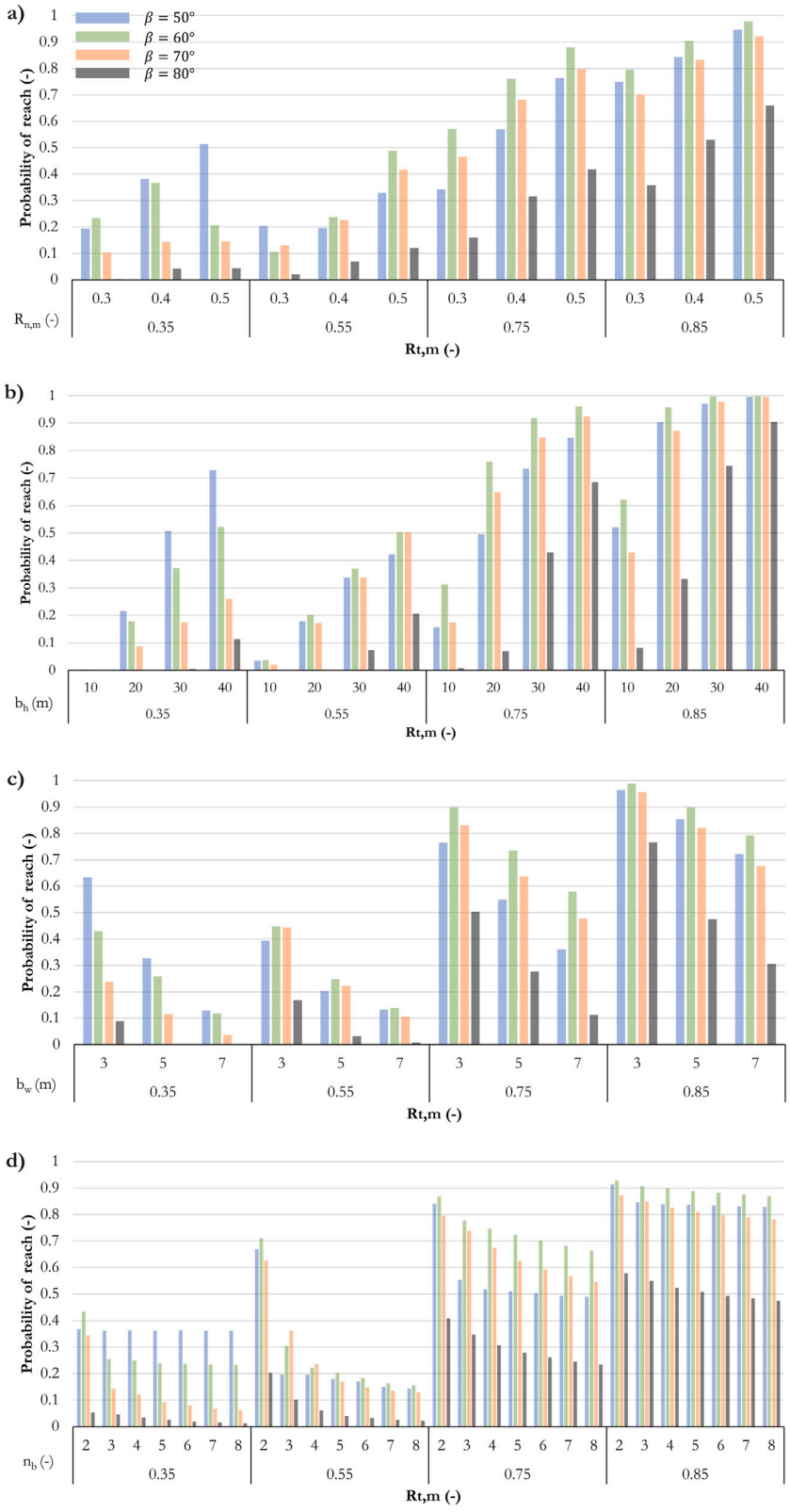

Fig. 5. Pivot charts of the number of arrival at the pit floor grouped according to the value for the tangential restitution coefficient $R_{t,m}$ and an additional variable ($R_{n,m}$, b_h, b_w, and n_b), as explained in the text and further divided by β.

$R_{t,m}$ = 0.35, $v_{h,95}$ spans from 10 to 20 m/s for all the configurations for which the blocks arrive. For $R_{t,m}$ = 0.85, values up to 60 m/s are observed increasing the number of benches. Referring to the velocity, a trend similar to that of Fig. 3 related to the distance is observed, except for the influence of bench angle β, which seems to be negligible. While blocks reach lower distances on the pit floor for decreasing β, the right tail of the distribution of the velocity, i.e. $v_{h,95}$, does not change as it reflects the velocity in the first impact on the floor. This behaviour

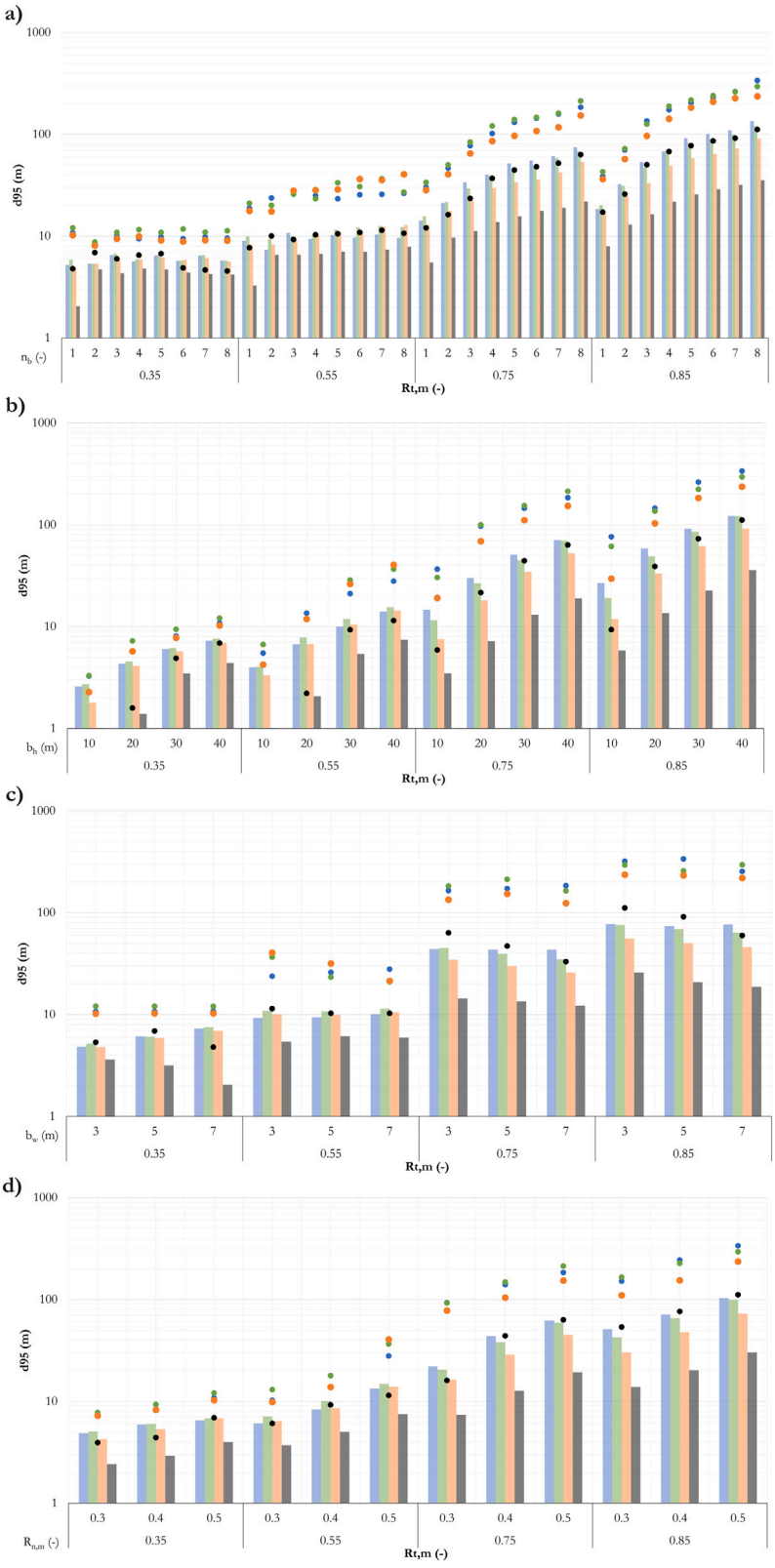

Fig. 6. Pivot charts of d_{95} at the pit floor: bar display the mean values, while points the maximum values, grouped according to the value for the tangential restitution coefficient $R_{t,m}$ as explained in the text and further divided by β.

confirms the fact that the slope angle affects the way the blocks are projected out of the face, while the falling height, thus the potential energy of the boulder, affects the velocity, i.e. the kinetic energy.

The linear fitting of the plots allows to appreciate an almost horizontal trend of $v_{h,95}$ for $R_{t,m} = 0.35$, regardless of $R_{n,m}$, while a slope equal to 0.15 and an intercept at around 13 m/s is found for

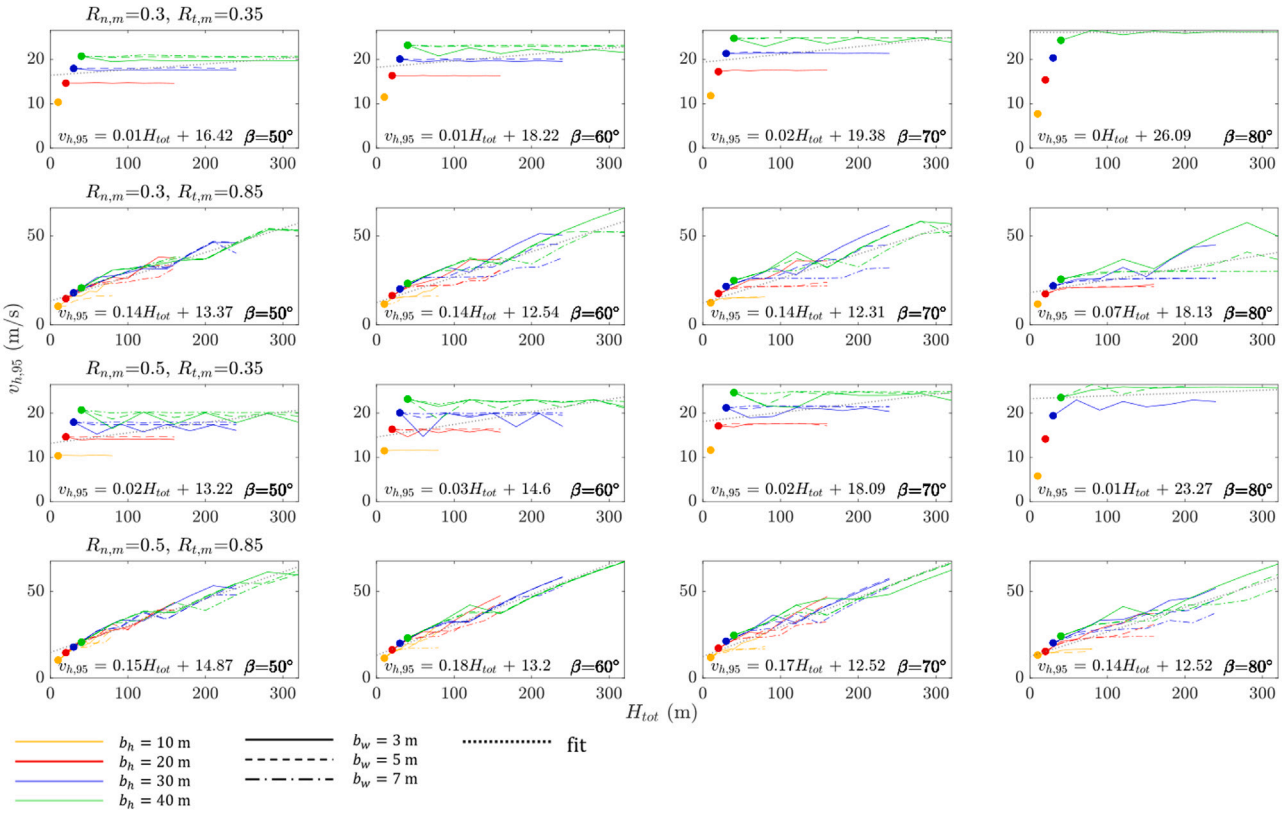

Fig. 7. Values of $v_{h,95}$ for different couples of $R_{n,m}$ and $R_{t,m}$, grouped for different values of β.

$R_{t,m} = 0.85$, independently from the bench angle. Table 3, reports the maximum values of $v_{h,95}$ for each materials couples. The worst (in terms of velocity) configuration presupposes a bench height of 40 m and a bench width of 3 m. Different number of benches are noted, as there are configurations for which blocks do not arrive on the pit floor.

Distance and velocity can be fitted with a line having equation

$$X = mH_{tot} + c, \tag{2}$$

where X is the observed parameter, m is the slope of the fitting line and c is its intercept, i.e. the value at $H_{tot} = 0$. Table 4 reports the values of m and c for all the studied configurations. Some consideration can be done:

- for $R_{t,m} \leq 0.55$, the equations

  $$d_{95} \sim 0.1H_{tot} + 4.45, \tag{3}$$

  and

  $$v_{h,95} \sim 0.2H_{tot} + 18.67, \tag{4}$$

  allow a rough and conservative estimation of d_{95} and $v_{h,95}$, even though for $\beta = 80°$ slightly different results can be displayed. It should be noted that these equations do not allow to define whether the blocks arrive, or not, on the pit floor.
- for $R_{t,m} > 0.55$, m and c varies according to $R_{n,m}$ and, for a given $R_{n,m}$, the case of $\beta = 80°$ shows different values, generally with a lower slope m and higher intercept c.

3.2. Mitigation measures

With the leading idea that controlling the geometry is not always possible or affordable, the kinematic parameters of the blocks along the bench edges were recorded in terms of characteristic values, i.e. h_{95} and $v_{v,95}$. Fig. 8 displays h_{95} and $v_{v,95}$, grouped with respect to the bench slope β. The way the results are presented is similar to what proposed for pit floor in Section 3.1. For sake of simplicity, two extreme cases are reported, only. The first two rows of Fig. 8 refer to $R_{n,m} = 0.3$, $R_{t,m} = 0.35$, the last two to $R_{n,m} = 0.5$, $R_{t,m} = 0.85$. The results display that $R_{t,m}$ is the most influencing parameter.

For low $R_{t,m}$, as observed in Fig. 4, the trajectories are similar for each bench. For this reason, a specific range of values can be found, almost irrespective of the number of benches n_b, except in those cases in which the blocks stop at the first bench. For a given β, the increase of b_w and the decrease of b_h promote the stop of the block at the first bench. This trend is further enhanced for large bench angles. Saw-tooth like curves refer to the fact that the position of the vertical recording section is fixed irrespective of the position of the bouncing of the bench. The obtained range of values of trajectory height h_{95} spans from 0 m, i.e. pure translational motion, up to 3 m high. The range for block velocity $v_{v,95}$ is between 2 m/s and 8.5 m/s. Despite the observed saw-tooth behaviours, an angular coefficient equal to 0 (horizontal line) for the linear fitting equation of h_{95} is generally observed for $R_{t,m} = 0.35$, while for $v_{v,95}$ its average value is around 0.01. On the contrary, for $R_{t,m} = 0.85$, the values are affected by the height and the number of benches. The influence of β is negligible, for both height and velocity, ss noted for the velocity at the pit floor.

3.3. Design charts

In order to provide a useful tool for the designers, the obtained results are organized in charts: for each material, four separate charts are realized for d_{95}, $v_{h,95}$, h_{95} and $v_{v,95}$, displaying the output values for each geometrical configuration. As for a given H_{tot}, different b_h values are possible by varying n_b, a different marker is adopted: circle, triangle, diamond and square for 10, 20, 30, 40 m high benches, respectively. The number of steps should be calculated according to b_h. On the x-axis, β values are provided, subdivided each for the possible b_w. According to the marker shape and position, a geometrical

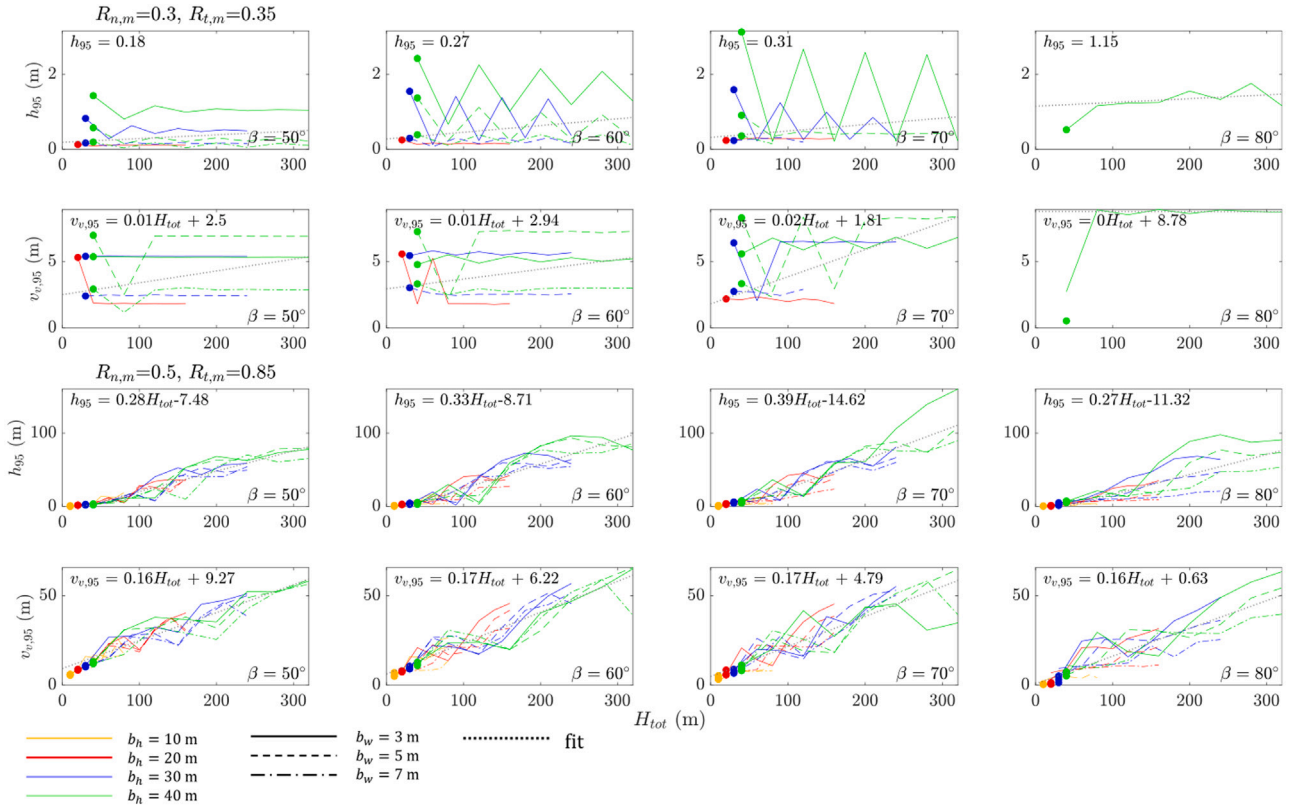

Fig. 8. Values of h_{95} and $v_{v,95}$ for different couples of $R_{n,m}$ and $R_{t,m}$, grouped for different values of β.

configuration is unequivocally determined. The markers are filled and their colour represents the output value. The colour bar associated to each plot defines the scale of the outputs. No-filled markers in $v_{h,95}$ represents the geometrical configurations for which blocks do not arrive on the pit. No-filled markers for d_{95} only, represents the case in which translational motion on the pit floor prevails. This information is particularly useful in those cases in which the geometry of the open pit is designed not to have blocks impacting on the pit floor. Values of $v_{v,95}$ and h_{95} can be used for a preliminary design of passive mitigation measures. Similarly as to the pit floor, $v_{v,95}$ chart allows to define, for each configuration, at which bench the blocks stop. As an example, Figs. 9 and 10 display the design charts for $R_{n,m}$ = 0.30 and $R_{t,m}$ = 0.85. Even though already displayed in Fig. 3, this chart allows to better appreciate that for b_h=10 m and b_w=7 m, except for n_b=1, no blocks arrive on the pit floor. In addition, d_{95} decreases for decreasing β. Considering together the charts of $v_{v,95}$ and h_{95}, it could be noted that for low values of β and b_h the translational motion prevails, as h_{95} = 0 is displayed, with a $v_{v,95}$ around 5 m/s.

The supplementary material reports all the charts for the all investigated materials.

An example of use is thus provided. It is assumed that a mining site has a material which can be classified (from a rockfall problem) with $R_{n,m}$ = 0.30 and $R_{t,m}$ = 0.85. To optimize productivity, the geometrical constraints are represented by $b_h \geq 20$ m and b_w equal to 7 m. Meanwhile, the geomechanical investigations highlight that a bench slope higher than 80° is not affordable for the stability. The maximum exploitable height H_{tot} is 60 m, i.e. n_b= 6 m with b_h = 10 m or n_b= 3 m with b_h = 20 m. With these limitation, Figs. 9 and 10 show that for all β values, considering h_b = 10 m, no blocks arrive on the pit and at each bench, except for the first bench that serves as collector of the falling blocks. Another use of the proposed charts is for the preliminary design of passive mitigation measures. Assuming that b_h = 20 m, b_w = 7 m and β = 70° have been selected for exploitation reasons, it could be noted that a $v_{v,95}$ from 5 m/s to 8 m/s can be reached in case of the detachment from the first bench and arrival on the second, third and fourth benches, with an increasing height up to 2.5 m. Supposing a rock block volume of 0.5 m^3 with a density of 2700 kg/m^3, it results a kinetic energy up to 43 kJ. It is worth mentioning that the presence of debris on the horizontal sections of the benches might considerably decrease both the run-out and the kinematic parameters of the eventually detached blocks and, in this case, dedicated analyses should be performed.

4. Conclusions

Rockfall represents an hazard both in mountainous region and in open pit mine contexts. In the latter case, the detachment and the fall of rock blocks constitutes a threat for workers and machinery and, consequently, both exploitation geometry and mitigation measures should be properly designed. To achieve such goals the knowledge of the characteristics and the kinematic parameters of the possible detached blocks is required. These lasts also depend on the material of the pit and the geometrical configuration, i.e. width, height, face angle, and number of benches. To tackle the problem, several parametric analyses of rockfall propagation in a hypothetical open pit context have been performed in the present work, through the use of synthetic two-dimensional profiles. The variation of all the above mentioned geometrical parameters has been investigated. In particular, a large number of trajectory analyses has been realized through a lumped-mass approach. This type of model, being independent from the mass of the released block, allows to properly scale the results according to the initial volume of the block. Thus, it can be tailored to each specific case. Different materials, considered representative of the possible scenarios, have been considered. In the framework of the Eurocodes, results are reported in terms of characteristic values, chosen as the 95th percentiles of their distributions. The reported outputs are:

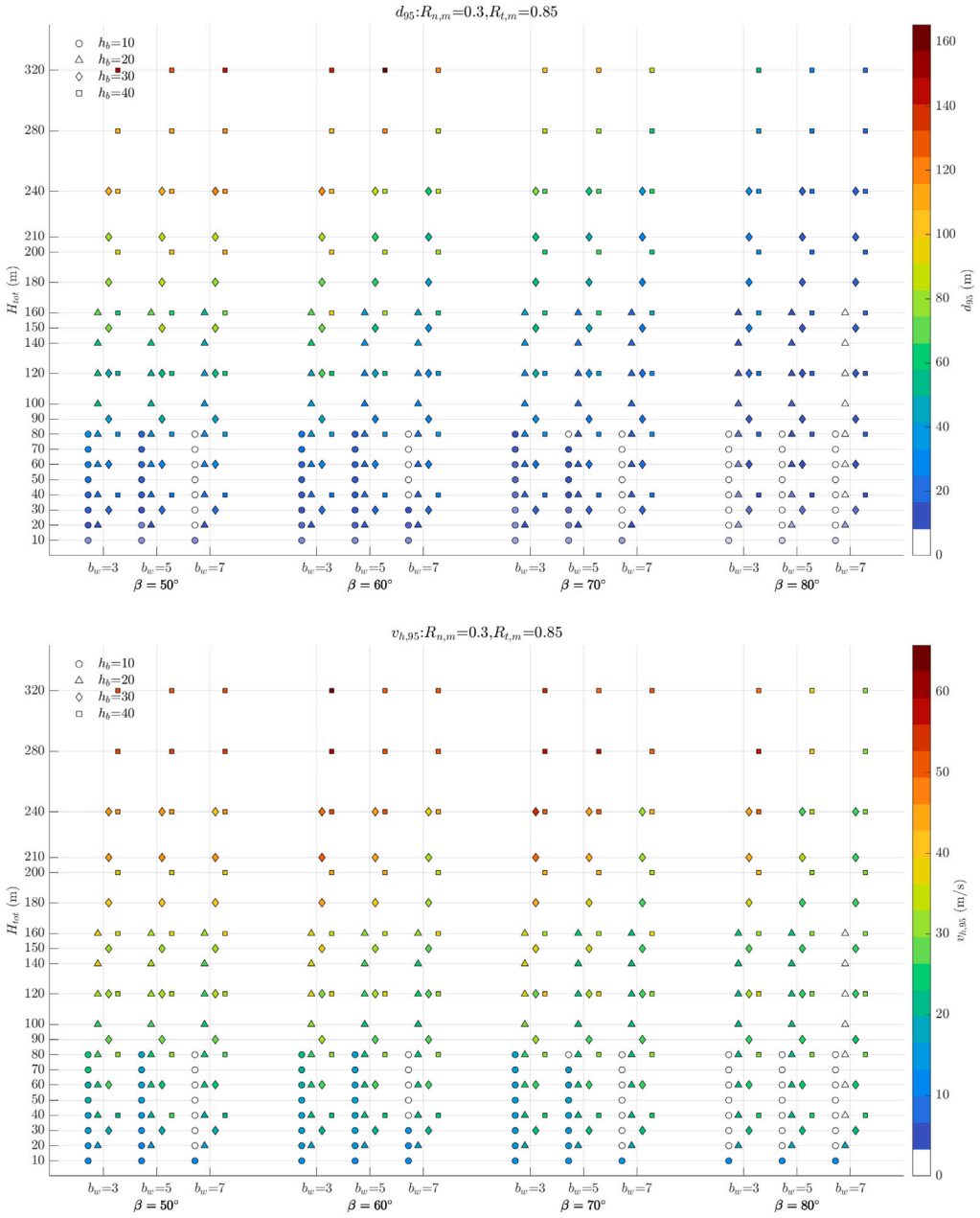

Fig. 9. Design charts of d_{95} and $v_{h,95}$ values for $R_{n,m} = 0.30$ and $R_{t,m} = 0.85$.

- run-out distance of the blocks on the pit floor;
- velocity of the blocks when impacting on the pit floor;
- passing height of the blocks recorded on each vertical section;
- velocity of the blocks recorded on each vertical section.

Aiming at providing a tool useful for a preliminary design of both pit geometry and mitigation measures, the results have been firstly analysed, grouped for materials, identified thanks to the normal and tangential restitution coefficients. Interesting findings have been observed:

- the tangential restitution coefficient seems to be the parameter that most affect the results. For values smaller than ≤ 0.55, the parameters related to the pit floor can be fitted by a horizontal line. For larger values, the linear fit increases its slope as function of the normal restitution coefficient for a bench angle smaller than 70°, while for steep slope ($\beta = 80°$) this trend is less evident and lower values of all the outputs are obtained;
- predictably, increasing bench width and/or increasing bench height, both run-out and kinematic parameters decrease;
- for all the materials, given bench height and width, very steep faces (80°) allows obtaining the lower blocks probabilities of reach on the pit floor. In case of low values of the restitution coefficients, no or negligible blocks arrive.

The results are reported in form of charts that can be used for the design of both pit geometry and passive mitigation measures. For each material, the output quantities are plotted as a function of the pit total height, for different geometrical configurations. The graph allows also individuating those configurations in which the blocks do not arrive either at the pit floor or at a specific bench.

The main limitations of this work relate with the disregard of the backbreak issue and the assumption of a unique material for the slope. Referring to the former, which generally tends to occur along pre-existing joints and blast-induced fractures, hazard assessment should

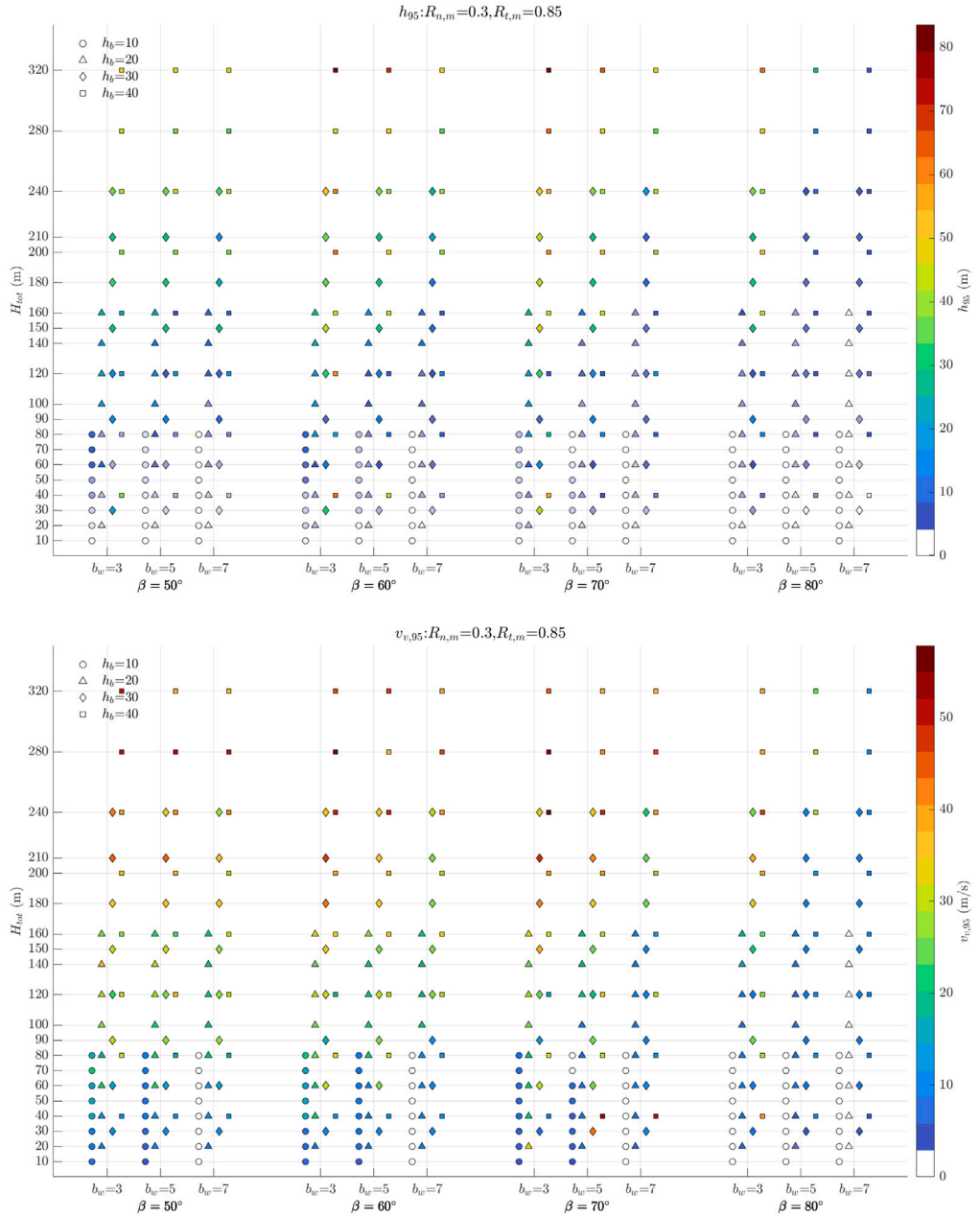

Fig. 10. Design charts of h_{95} and $v_{v,95}$ values for $R_{n,m}$ = 0.30 and $R_{t,m}$ = 0.85.

consider that the real bench geometry could differ from the ideal designed one. To overcome this limitation in the design phase, as proposed by Alejano et al.,[35] the estimated minimum recommended bench width could be increased by a value representing the average expected backbreak, about 0.5 m for pre-split benches, 1 m for carefully blasted good-quality rock masses, and 2 m for less carefully blasted average-quality rock masses. With regard to the second aspect, future works can consider different materials in the same working site, with particular reference to the presence of debris on the benches. Different statistical distributions for the material parameters can also be investigated.

It should be also stressed that our charts technique provides average values for well-managed quarries, while, given the variable nature of rock masses, there may be more complex cases in which site-specific studies must be performed. Nevertheless, for the preliminary open pit design, for a quantitative rockfall risk assessment and for the eventual design of protective measures, the provided charts and equations can be considered an effective tool.

Declaration of competing interest

The authors declare that they have no known competing financial interests or personal relationships that could have appeared to influence the work reported in this paper.

Data availability

Data will be made available on request.

Acknowledgements

This research was partially supported by the Australian Research Council (DP210101122) and partially supported by the PNRR NODES project “Nord Ovest Digitale E Sostenibile”, funded by the MUR—M4C2 1.5 of PNRR program (n° ECS00000036).

Table 4
Regression coefficients for d_{95} and $v_{h,95}$ recorded at the pit floor for all the configurations.

$R_{t,m}$	$R_{n,m}$	β	d_{95}		$v_{h,95}$	
			m	c	m	c
0.35	0.3	50	0.007	4.05	0.013	16.42
0.35	0.3	60	0.007	4.05	0.014	18.22
0.35	0.3	70	0.003	4.03	0.018	19.38
0.35	0.3	80	0.000	3.71	0.000	26.09
0.35	0.4	50	0.007	4.97	0.013	15.77
0.35	0.4	60	0.007	4.94	0.017	17.09
0.35	0.4	70	0.006	4.52	0.016	19.48
0.35	0.4	80	0.001	3.91	0.015	22.46
0.35	0.5	50	0.015	4.31	0.023	13.22
0.35	0.5	60	0.016	4.42	0.028	14.60
0.35	0.5	70	0.012	5.08	0.021	18.09
0.35	0.5	80	−0.002	5.35	0.006	23.27
0.55	0.3	50	0.010	4.55	0.016	14.52
0.55	0.3	60	0.020	4.05	0.026	15.24
0.55	0.3	70	0.011	4.94	0.015	18.71
0.55	0.3	80	0.001	4.37	0.005	22.83
0.55	0.4	50	0.030	4.00	0.027	12.30
0.55	0.4	60	0.037	5.02	0.031	14.18
0.55	0.4	70	0.024	5.17	0.031	16.76
0.55	0.4	80	0.001	5.68	0.007	22.57
0.55	0.5	50	0.062	5.37	0.036	11.95
0.55	0.5	60	0.065	6.43	0.047	13.64
0.55	0.5	70	0.082	3.00	0.066	14.08
0.55	0.5	80	0.012	6.66	0.022	21.31
0.75	0.3	50	0.166	0.76	0.081	12.74
0.75	0.3	60	0.151	1.18	0.072	16.21
0.75	0.3	70	0.122	0.51	0.073	16.24
0.75	0.3	80	0.024	4.20	0.028	22.20
0.75	0.4	50	0.389	−3.02	0.111	13.47
0.75	0.4	60	0.353	−4.57	0.116	13.80
0.75	0.4	70	0.263	−3.64	0.115	13.60
0.75	0.4	80	0.070	2.83	0.058	19.88
0.75	0.5	50	0.559	−1.57	0.134	12.90
0.75	0.5	60	0.574	−7.27	0.145	13.04
0.75	0.5	70	0.417	−5.07	0.145	12.84
0.75	0.5	80	0.138	1.28	0.101	15.36
0.85	0.3	50	0.457	0.00	0.137	13.37
0.85	0.3	60	0.412	0.00	0.143	12.54
0.85	0.3	70	0.282	0.00	0.137	12.31
0.85	0.3	80	0.082	0.00	0.071	18.13
0.85	0.4	50	0.644	0.00	0.144	14.41
0.85	0.4	60	0.651	0.00	0.165	12.28
0.85	0.4	70	0.484	0.00	0.162	12.05
0.85	0.4	80	0.165	0.00	0.117	13.81
0.85	0.5	50	0.934	0.00	0.155	14.87
0.85	0.5	60	0.938	0.00	0.176	13.20
0.85	0.5	70	0.760	0.00	0.171	12.52
0.85	0.5	80	0.279	0.00	0.142	12.52

Appendix A. Code validation

The trajectory code written by the Authors implements the well-known equations of the motion under the lumped-mass model assumption. As detailed in the theoretical documents of RocFall software,[42] three types of motions are considered: free fall, bouncing, and translation (sliding). The approach does not account for the block shape and the mass serves to compute the energy, only. The block is considered point-like and the slope profile is discretized into segments.

The projectile algorithm is used to compute blocks motion in air: through this algorithm the location of intersection between the flying trajectory of the rock and a slope segment is found. Once the intersection point is found, the post-impact impact velocity (in terms of magnitude and direction) is calculated according to the pre-impact velocity and the coefficients of restitution. If, after the impact, the blocks fulfil specific requirements, defined below, the process begins again, with the search for next intersection point. Otherwise, the blocks start to slide or stop. Sliding velocity along the path is regulated by the ratio between the inclination of the slope segment θ and the friction angle ϕ: if $\theta = \phi$, the velocity does not change until the end of the segment; if $\theta > \phi$, block velocity increases; if $\theta < \phi$, the velocity decreases and a stopping distance, assuming a segment infinitely long, is calculated. This distance is compared with the remaining length on the segment: if the stopping distance is greater than the distance to the end of the segment, then the block will slide off of the end of the segment, otherwise it stops before the end. Velocity increase or decrease is proportional to the distance between the block and the end of the segment, the block in-going velocity direction, and it is a function of θ and ϕ values, as detailed in Ref. 42

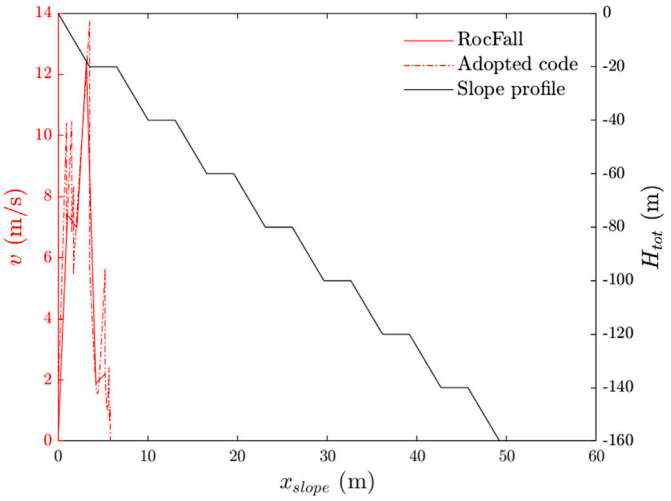

Fig. A.11. Comparison between the results obtained with RocFall v017 and the code developed by the Authors in terms of the velocity of the block.

As mentioned before, velocity threshold values and/or particular conditions have to be set to determine: (i) the transition between bouncing and sliding (and vice-versa), (ii) when bouncing blocks are considered stopped. With reference to the former, the Authors considered that a threshold value on the modulus of the velocity, only, is not able to catch the case in which blocks are sliding with high velocity along the slope. Thus, the Authors assumed that transition from bouncing to sliding occurs (i) if the velocity in modulus is under a threshold value defined equal to 1 m/s and (ii) if the component normal to the slope is smaller than a threshold value set equal to 0.05 m/s. Referring to the second problem, a block stops when its velocity reaches a threshold velocity value, in modulus, of 0.01 m/s. Some other refinements are inserted to avoid numerical instabilities, e.g. infinite vertical rebound on an horizontal segment.

To validate the code, a comparison with RocFall v017 was made, both in deterministic and probabilistic frameworks, i.e. with deterministic values for the input parameters in the first case and randomly selected with a Monte-Carlo sampling method in the second. The geometric configuration $b_h = 20$ m, $b_w = 3$ m, $\beta = 80°$ and $n_b = 8$ is taken as an example. The restitution coefficients $R_{n,m}$ and $R_{t,m}$ are set equal to 0.4 and 0.65, respectively. The friction angle is set to 30°. In the deterministic analysis, no standard deviation is assigned to the input parameters. Fig. A.11 reports the value of the velocity v along the slope profile obtained in the analyses with the Authors code and RocFall. Both the values of v and the stopping distance are in a very good agreement, as displayed in Fig. A.12.a which allows to compare quantitatively the obtained trajectories.

The same configuration is considered for performing probabilistic trajectory analyses, associating the standard deviations to the input parameters as in Table 2. Table A.5 reports the obtained outputs in terms of v_{95}, h_{95}, d_{95}, and number of impacts. A good accordance among the results emerges, as also highlighted in Fig. A.12.b, displaying the obtained trajectories.

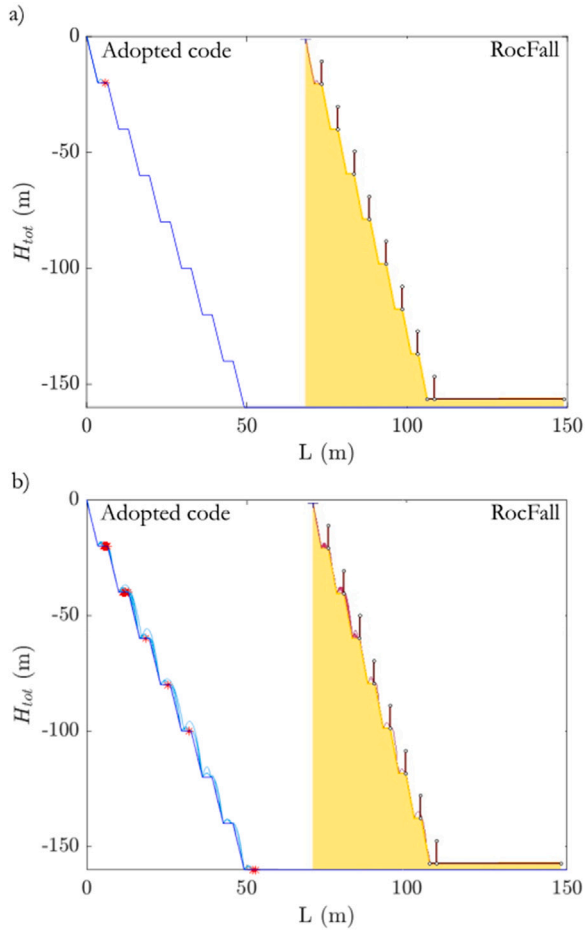

Fig. A.12. Comparison between the results obtained with RocFall v017 and the code developed by the Authors for the deterministic (a) and the probabilistic (b) analyses.

Table A.5
Comparison between the results obtained with RocFall v017 and the code developed by the Authors in terms of $v_{v,95}$, h_{95}, $v_{h,95}$, and d_{95} (herein expressed as h_{95} at the pit bottom), and number of impact n_{impact}.

	RocFall			Adopted code		
Bench	h_{95} (m)	v_{95} (m/s)	n_{impact}	h_{95} (m)	v_{95} (m/s)	n_{impact}
1	2.10	0.2	11	2.10	0.2	11
2	6.56	1.18	9	6.57	1.18	9
3	3.13	0.12	2	3.13	0.13	3
4	2.98	0.14	2	3.00	0.15	2
5	2.71	0.1	1	2.72	0.1	2
6	0.52	0.04	1	0.51	0.01	2
7	5.76	1.46	1	5.76	1.47	1
Pit floor	2.36	0.4	3	2.38	0.4	3

It should be noticed that very few blocks arrive on the pit floor. In the present work, the analyses for which less than the 1% of blocks arrives at the location of the collectors were not considered. This choice agrees (i) with the assumption that a very low acceptable residual risk value can be accepted and (ii) with the probabilistic design approach for which it is assumed that in the distribution of the effects of the actions a very low percentile exceeds the characteristic value of the resistance.

Appendix B. Supplementary data

Supplementary material related to this article can be found online at https://doi.org/10.1016/j.ijrmms.2023.105551.

References

1. Hungr O, Leroueil S, Picarelli L. The Varnes classification of landslide types, an update. *Landslides*. 2014;11(2):167–194.
2. Scavia C, Barbero M, Castelli M, Marchelli M, Peila D, Torsello G, Vallero G. Evaluating rockfall risk: Some critical aspects. *Geosciences*. 2020;10(3):98.
3. Coli M, Pini G, Cantini C. Hazard evaluation of rock-fall induced by quarry-blasting. In: *ISRM international symposium-5th Asian rock mechanics symposium*. OnePetro; 2008:066.
4. Macciotta R, Altamirano F, Gibbins L, Espezua M, Fernández R, Maguiña J. Rock fall hazard analysis for in-pit operations potentially impacting External Sensitive Areas. *Mining*. 2021;1(2):135–154.
5. Read J, Stacey P. *Guidelines for open pit slope design*. CSIRO publishing; 2009.
6. Darling P. *SME mining engineering handbook, Vol. 1*. SME; 2011.
7. Hustrulid W, Kuchta M. *Open pit mine planning and design. volume 1-fundamentals*. Balkema; 2013.
8. Ferrari F, Thoeni K, Giacomini A, Lambert C. A new rockfall hazard assessment methodology for open-pit coal mines. In: *Bowen basin symposium*. 2015:355–362.
9. Ferrari F, Giacomini A, Thoeni K. *Qualitative rockfall hazard assessment: a comprehensive review of current practices*. 2016:2865—2922.
10. Ferrari F, Giacomini A, Thoeni K, Lambert C. Qualitative evolving rockfall hazard assessment for highwalls. *Int J Rock Mech Min Sci*. 2017;98:88–101.
11. Alejano L, Stockhausen H, Alonso E, Bastante F, Oyanguren PR. ROFRAQ: A statistics-based empirical method for assessing accident risk from rockfalls in quarries. *Int J Rock Mech Min Sci*. 2008;45(8):1252–1272.
12. Falanesca M, Borio L, Picchio A, Peila D. QuaRRi: a new methodology for rock-fall risk analysis and management in quarry exploitation. *Gospod Surowcami Miner*. 2010;26:149–161.
13. Peila D, Patrucco M, Falanesca M. Quantification and management of rockfall risk in opencast quarrying activities. *Environ Eng Geosci*. 2011;17(1):39–51.
14. Peila D, Oggeri C. The use of rockfall protection systems in surface mining activity. *Int J Surf Min Reclam Environ*. 2003;17(1):51–64.
15. Thoeni K, Giacomini A, Sloan S, Lambert C, Casagrande D. Numerical analysis of rockfall hazard in open pit coal mines. In: *13th international conference of the IACMAG 2011*. University of Canterbury. Civil and Natural Resources Engineering; 2011:1151–1156.
16. Giacomini A, Thoeni K, Lambert C, Booth S, Sloan S. Experimental study on rockfall drapery systems for open pit highwalls. *Int J Rock Mech Min Sci*. 2012;56:171–181.
17. Thoeni K, Giacomini A, Lambert C, Sloan SW, Carter JP. A 3D discrete element modelling approach for rockfall analysis with drapery systems. *Int J Rock Mech Min Sci*. 2014;68:107–119.
18. Hutchison B, Morrison A, Lucas D. *Steep wall mining: engineered structures used in the management of rockfall hazards at Kanmantoo copper mine*. Australia: Australian Centre for Geomechanics: Perth; 2020:831–848.
19. De Biagi V, Marchelli M, Peila D. Reliability analysis and partial safety factors approach for rockfall protection structures. *Eng Struct*. 2020;213:110553.
20. Marchelli M, De Biagi V, Peila D. Reliability-based design of rockfall passive systems height. *Int J Rock Mech Min Sci*. 2021;139:104664.
21. Harries N, Noon D, Pritchett H, Bates D. Slope stability radar for managing rock fall risks in open cut mines. In: *Rock engineering in difficult conditions, proceedings of the 3rd canada–us rock mechanics symposium*. 2009:9–15.
22. Robiati C, Eyre M, Vanneschi C, Francioni M, Venn A, Coggan J. Application of remote sensing data for evaluation of rockfall potential within a quarry slope. *ISPRS Int J Geo-Inf*. 2019;8(9):367.
23. Giacomini A, Thoeni K, Santise M, Diotri F, Booth S, Fityus S, Roncella R. Temporal-spatial frequency rockfall data from open-pit highwalls using a low-cost monitoring system. *Remote Sens*. 2020;12(15):2459.
24. Michelini A, Viviani F, Bianchetti M, Coli N, Leoni L, Stopka C. A new radar-based system for detecting and tracking rockfall in open pit mines. In: *Slope stability 2020: proceedings of the 2020 international symposium on slope stability in open pit mining and civil engineering*. Australian Centre for Geomechanics; 2020:1183–1192.
25. Lanciano C, Salvini R. Monitoring of strain and temperature in an open pit using Brillouin distributed optical fiber sensors. *Sensors*. 2020;20(7):1924.
26. Ryan TM, Pryor PR. Designing catch benches and interramp slopes. *Slope Stab Surf Min*. 2000:27–38.
27. Hartman HL, Britton SG, Mutmansky JM, Gentry DW, Schlitt WJ, Karmis M, Singh MM. *SME mining engineering handbook, Vol. 2*. Society for Mining, Metallurgy, and Exploration Denver; 1992.
28. Gibson W, De Bruyn I, Walker D. Considerations in the optimisation of bench face angle and berm width geometries for open pit mines. In: *International symposium on stability of rock slopes in open pit mining and civil engineering*. Johannesburg: The South African Institute of Mining and Metallurgy; 2006:557–578.
29. Gumede T. Measurement of typical joint characteristics in South African gold mines and the use of these characteristics in the prediction of rock falls. *J South Afr Inst Min Metall*. 2007;107(5):335–344.
30. Dimitrakopoulos R, Farrelly C, Godoy M. Moving forward from traditional optimization: grade uncertainty and risk effects in open-pit design. *Min Technol*. 2002;111(1):82–88.

31. Ritchie AM. *Evaluation of rockfall and its control*. Tech. rep. 17; Highway research record; 1963.
32. Pierson LA, Gullixson CF, Chassie RG, et al *Rockfall catchment area design guide: final report: metric edition*. Tech. rep.; Oregon. Dept. of Transportation. Research Group; 2001.
33. Giacomini A, Thoeni K, Kniest E, Lambert C. In situ experiments of rockfall in an open pit coal mine. *Proc Slope Stab*. 2011:1–11.
34. Peila D, Fornaro M. La gradonatura del fronte di cava quale elemento di protezione dalla caduta di blocchi sul piazzale: analisi cinematica del fenomeno per differenti configurazioni. *Boll Assoc Miner Subalp*. 1987;Year XXIV(34):329–339.
35. Alejano L, Pons B, Bastante F, Alonso E, Stockhausen H. Slope geometry design as a means for controlling rockfalls in quarries. *Int J Rock Mech Min Sci*. 2007;44(6):903–921.
36. Ferrari F, Thoeni K, Giacomini A, Lambert C. A rapid approach to estimate the rockfall energies and distances at the base of rock cliffs. *Georisk: Assess Manage Risk Eng Syst Geohazards*. 2016;10(3):179–199.
37. Chai B, Tang Z, Zhang A, Du J, Su H, Yi H. An uncertainty method for probabilistic analysis of buildings impacted by rockfall in a limestone quarry in Fengshan, Southwestern China. *Rock Mech Rock Eng*. 2015;48(5):1981–1996.
38. Preh A, Mitchell A, Hungr O, Kolenprat B. Stochastic analysis of rock fall dynamics on quarry slopes. *Int J Rock Mech Min Sci*. 2015;80:57–66.
39. Saroglou H, Bar N. Predicting the primary impact and total rollout distances of rock falls based on cases in quarries and mines in Australia and the United Kingdom. In: *51st US rock mechanics/geomechanics symposium*. OnePetro; 2017:401.
40. Evans CL. *The design of catch bench geometry in surface mines to control rockfall*. The University of Arizona; 1989.
41. Utili S, Agosti A, Morales N, Valderrama C, Pell R, Albornoz G. Optimal Pitwall shapes to increase financial return and decrease carbon footprint of open pit mines. *Min Metall Explor*. 2022;39(2):335–355.
42. RocScience Inc. RocFall, user's guide. 1998–2002.
43. Li L, Lan H. Probabilistic modeling of rockfall trajectories: a review. *Bull Eng Geol Environ*. 2015;74(4):1163–1176.
44. EN 1990:2002. Eurocode 0 - Basis of structural design. 2002.
45. EN 1997-1:2004. Eurocode 7 - geotechnical design. Part 1: General rules. 2004.
46. UNI 11211-4. Opere di difesa dalla caduta massi - Parte 4: Progetto definitivo ed esecutivo. 2018.
47. Miller SM, Girard JM, McHugh E. Computer modeling of catch benches to mitigate rockfall hazards in open pit mines. In: *4th North American rock mechanics symposium*. OnePetro; 2000:1–6.
48. Asteriou P, Saroglou H, Tsiambaos G. Geotechnical and kinematic parameters affecting the coefficients of restitution for rock fall analysis. *Int J Rock Mech Min Sci*. 2012;54:103–113.
49. Pfeifer TJ, Bowen TD. Computer simulation of rockfalls. *Bull Assoc Eng Geol*. 1989;26(1):135–146.
50. Giani G. *Rock slope stability analysis*. Balkema; 1992.
51. Robotham M, Wang H, Walton G. Assessment of risk from rockfall from active and abandoned quarry slopes. 1995:237A. 5,
52. Chau KT, Wong R, Wu J. Coefficient of restitution and rotational motions of rockfall impacts. *Int J Rock Mech Min Sci*. 2002;39(1):69–77.
53. Crosta G, Agliardi F. A methodology for physically based rockfall hazard assessment. *Nat Hazards Earth Syst Sci*. 2003;3(5):407–422.
54. Spadari M, Giacomini A, Buzzi O, Fityus S, Giani G. In situ rockfall testing in new south wales, australia. *Int J Rock Mech Min Sci*. 2012;49:84–93.
55. Piteau D, Clayton R. Computer rockfall model. In: *Meeting on rockfall dynamics and protective works effectiveness*. Bergamo; 1987:123–125.
56. Guzzetti F, Crosta G, Detti R, Agliardi F. STONE: a computer program for the three-dimensional simulation of rock-falls. *Comput Geosci*. 2002;28(9):1079–1093.
57. Bourrier F, Berger F, Tardif P, Dorren L, Hungr O. Rockfall rebound: comparison of detailed field experiments and alternative modelling approaches. *Earth Surf Process Landf*. 2012;37(6):656–665.
58. Frattini P, Crosta GB, Valagussa A. Rockfall runout modelling for hazard characterization and countermeasure design in urban area. In: *Landslide science for a safer geoenvironment: volume 3: targeted landslides*. Springer; 2014:385–391.